Heliyon 6 (2020) e05277

Contents lists available at ScienceDirect

Heliyon

journal homepage: www.cell.com/heliyon

Research article

Quasiphonon polaritons

Lu Cheng, Wei Zheng *, Lemin Jia, Feng Huang

State Key Laboratory of Optoelectronic Materials and Technologies, School of Materials, Sun Yat-sen University, Guangzhou 510275, China

ARTICLE INFO

Keywords:
Condensed matter physics
Electromagnetism
Materials science
Optics
Optical anisotropy
Birefringence
Quasiphonon polaritons
Reststrahlen band

ABSTRACT

Mid-infrared reflection spectra of *c*- and *m*-plane bulk AlN show a reststrahlen band related to the formation of phonon polaritons. However, it is worth noting that there are additional hump- and spike-shaped peaks in the spectra, which cannot be explained by the phonon-polaritons model applicable to optically isotropic crystals. Here, considering the existence of quasiphonons in wurtzite crystals, we suppose that the extra peaks result from the generation of quasiphonon polaritons (QPPs) induced by the coupling between photon and quasi-transverse optical phonon. On the basis of this point, a QPPs model applicable to optically anisotropic wurtzite crystals is developed, which successfully explains the reststrahlen band of bulk AlN. Besides, on the ground of our model, a series of reststrahlen band of bulk AlN under various configurations is also predicted and presented.

1. Introduction

Different kinds of macroscopic symmetries of crystals are induced by the periodic arrangement of atoms in crystals, which not only result in different geometry appearance of crystals but also in the anisotropy of the macroscopic physical properties of crystals [1]. When it comes to the optical property of crystals, in particular, a circumstance called birefringence has been found early [2], that is, when a monochromatic light refracts at the air-crystal interface, two refracted lights will propagate in this crystal, of which the reason is that different symmetries of crystals contribute to the anisotropy of the dielectric function of crystals. According to specific symmetry, crystals with different optical properties can be classified into three catagories: cubic crystal, uniaxial crystal and biaxial crystal. For uniaxial crystal, the two refracted lights propagate in it are known as ordinary ray (*o* ray) and extraordinary ray (*e* ray), which are the subjects widely studied [3, 4, 5, 6].

In polar crystals, the vibration of polar lattice results in the interaction of photon and transverse optical (TO) phonon, which brings the well-known phonon polaritons, and then a photonic band gap known as reststrahlen band with the characteristic of strong reflectance will appear [7]. However, there are two points worthy of attention. On the one hand, the widely used phonon-polaritons model [8, 9] and the interface reflectance formulas [2] are only suitable for optically isotropic crystals like cubic crystals. On the other hand, optical anisotropy means that the reststrahlen band of polar crystals is also anisotropic, and accordingly, additional peaks may arise on the reststrahlen band [10, 11], which cannot be well explained or analyzed by the original phonon-polaritons model.

Wurtzite structure is one of the simplest structures of uniaxial crystals. According to group theory, in wurtzite crystals, A_1 phonon is polarized along the optical axis and it can be infrared activated when *e* ray propagates in the crystal; E_1 phonon is polarized in the plane perpendicular to the optical axis, and its infrared activity can be observed when *o* ray propagates [12, 13]. Previous studies showed that when the long-range electrostatic forces in wurtzite crystals exceed the short-range interatomic forces, an obvious frequency gap between TO and LO phonons will occur [14]. Then the quasi-TO (or quasi-LO) phonons may be generated by the possible mixing of pure TO (or LO) phonons of different symmetries in a comparatively narrow frequency range [15, 16, 17, 18], from which we can speculate that the extra peaks on the reststrahlen band of wurtzite crystals may be relevant to the generation of quasi-TO phonon, which can couple with photon to form a polariton different from that in the optically isotropic crystal.

As a representative wurtzite polar semiconductor with an ultrawide direct bandgap of about 6.2 eV, Aluminum nitride (AlN) has attracted great attention with its unique optical properties and potential for optoelectronic devices [19, 20, 21, 22, 23, 24]. Here, the reststrahlen band of AlN was analyzed and discussed in detail. Firstly, the general reflectance formulas for uniaxial crystals based on a comprehensive consideration of the incident angle and polarization state of the incident light was deducted. Then, considering the presence of quasiphonons in wurtzite crystals, we developed a quasiphonon-polaritons (QPPs) model applicable for optically anisotropic wurtzite crystals. Finally, explanation and further forecast to the reststrahlen band of bulk AlN relevant to the quasiphonon polaritons under different conditions of crystal facets have

* Corresponding author.
E-mail address: zhengw37@mail.sysu.edu.cn (W. Zheng).

https://doi.org/10.1016/j.heliyon.2020.e05277
Received 30 August 2020; Received in revised form 21 September 2020; Accepted 12 October 2020

therefore been conducted. All the above researches help to gain a better understanding of the optical anisotropy of wurtzite crystals.

2. Materials and methods

2.1. Sample preparation

The *c*- and *m*-plane AlN bulk single crystals were obtained by physical vapor transport (PVT) method in a tungsten (W) crucible under a high-purity nitrogen ambience with high growth temperature of 2100–2400 °C controlled by a resistive-heating system. The crystal facets were polished to be smooth (as shown in Figure 1) for the spectral measurements.

2.2. Spectral measurements

Mid-infrared reflection spectra of *c*- and *m*-plane AlN were measured via Fourier Transform Infrared Spectrometer (IRAffinity-1S), of which the light source was non-polarized natural light. The measuring range was from 400 to 4000 cm^{-1} with the incident angle fixed as 10°. A gold mirror was used for background scanning in the measurement.

3. Results and discussion

3.1. Mid-infrared reflection spectra of c- and m-plane bulk AlN

Figure 1 presents the experimental mid-infrared reflection spectra of *c*- and *m*-plane bulk AlN, from which a reststrahlen band similar to that caused by phonon-polaritons effect can be observed in the range of 400–1000 cm^{-1}, which can also be observed in wurtzite ZnO [25]. It is worth noting that the experimental reflection curves are not smooth with additional characteristic peaks showing up at high or low frequency, that is, a hump- and a spike-shaped peak appear on the reflection curve of *c*- and *m*-plane AlN, respectively.

3.2. Fitting by phonon-polaritons model

In order to explain the extra characteristic peaks shown in the experimental reflection curve of *c*- and *m*-plane AlN, the widely used phonon-polaritons model is taken into consideration, which yields the dielectric function as [8, 9, 26, 27]:

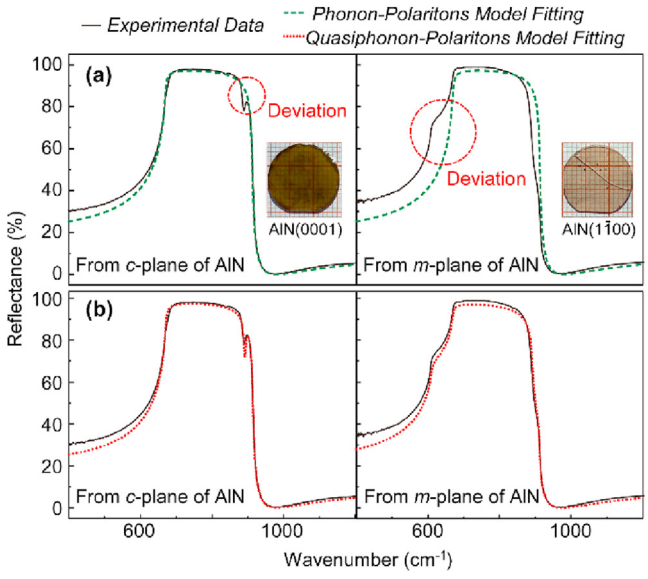

Figure 1. Experimental data (solid lines) of *c*- and *m*-plane bulk AlN and two theoretical fitting models. (a) Phonon-polaritons model (green dashed lines); (b) Quasiphonon-polaritons model (red short-dashed lines).

$$\varepsilon = \varepsilon_\infty + \sum_j \frac{\omega_{TOj}^2 S_j}{\left(\omega_{TOj}^2 - \omega^2 - i\omega\gamma_j\right)}, \tag{1}$$

where j is the number of a vibration mode with specific symmetry, ε_∞ and ε_s are the high- and low-frequency dielectric constants, respectively, S is the mode strength and there is $\varepsilon_s = \varepsilon_\infty + \sum_{j=1} S_j$, ω_{TO} is the TO phonon wavenumber with γ as its damping constant. For AlN, at the symmetry point Γ of the Brillouin zone, there is $\Gamma^{optical} = A_1 + E_1 + 2B_1 + 2E_2$ for optical phonon mode symmetry, where A_1 and E_1 are both infrared active [28] and thus j in Eq. (1) is 1.

For optically isotropic crystals, the interface reflectance formulas can be derived from Maxwell's equation when the electric field vector of incident linearly polarized light is perpendicular or parallel to the incident plane (assuming that the light is incident from air to the crystal surface) [2]:

$$R_s = \left| \frac{\cos\theta_i - \sqrt{\varepsilon - \sin^2\theta_i}}{\cos\theta_i + \sqrt{\varepsilon - \sin^2\theta_i}} \right|^2, \tag{2}$$

$$R_p = \left| \frac{\varepsilon\cos\theta_i - \sqrt{\varepsilon - \sin^2\theta_i}}{\varepsilon\cos\theta_i + \sqrt{\varepsilon - \sin^2\theta_i}} \right|^2, \tag{3}$$

where θ_i is the incident angle. If the electric field vector $\mathbf{E}$ of the incident light has a certain angle ϕ (from 0° to 90°) to the incident plane, the interface reflectance will include contributions from both perpendicular and parallel polarization:

$$R = \left| \frac{\mathbf{E}_r}{\mathbf{E}_i} \right|^2 = R_s \sin^2\phi + R_p \cos^2\phi. \tag{4}$$

In particular, for natural light, the reflectance can be expressed as $R_{mix} = (R_s + R_p)/2$ because the energy of light wave is equal in the two orthogonal components.

Considering that the incident angle here is fixed as 10° and the light source of FTIR spectrometer is natural light, we calculate the reststrahlen band described by phonon-polaritons model (the green dashed lines shown in Figure 1(a)). The dielectric function corresponding to E_1 phonon of AlN is used in this model [28, 29]. The specific parameters of E_1 phonon are $\omega_{TO} = 670\ cm^{-1}$, $\gamma_{TO} = 5.2\ cm^{-1}$, $\varepsilon_s = 7.28$ and $\varepsilon_\infty = 3.93$, respectively. Considering that the incident angle here is fixed as 10° and the light source of FTIR spectrometer is non-polarized natural light, we first calculate R_s and R_p through Eqs. (2) and (3) corresponding to E_1 phonon, and then the reflectance of natural light is obtained via Eq. (4).

It can be seen that the curves given by this model have large discrepancy with the experimental results, especially in the positions of the hump- and spike-shaped peaks, of which the reason is obvious: on one hand, the process of deriving dielectric function contributed by the phonon polaritons described in Eq. (1) is simplified by an assumption that the crystal has a cubic symmetry [8]; on the other hand, the interface reflectance described in Eqs. (2) and (3) is only valid when light is reflected at the interface between two isotropic media. For cubic crystal with high macroscopic symmetry, its dielectric function is a scalar, i.e., its optical properties are isotropic, so Eqs. (1), (2), and (3) are suitable for describing its optical properties. However, for hexagonal crystals such as AlN, the symmetry of the crystal is obviously not as high as that of cubic crystals. At this time, the dielectric function is in tensor form, and thus the optical properties of the crystals will show anisotropy, which means that the phonon-polaritons model described by Eqs. (1), (2), and (3) is no longer applicable to analyzing its reststrahlen band, let alone explaining the additional characteristic peaks.

3.3. Fitting by quasiphonon-polaritons model

In order to describe the reststrahlen band of optically anisotropic crystals, we need to modify Eqs. (1), (2), and (3) and establish a new

model called quasiphonon-polaritons model. The following discussion only targets the uniaxial crystals with the crystal *c*-axis as optical axis. Figure 2 presents the general situation of reflectance measurement on an arbitrarily orientated crystal facet of a uniaxial crystal. A fixed laboratory coordinate system o - $\xi\eta\zeta$, which is independent of crystallography coordinate system, is established on the crystal facet measured in the experiment. The $\xi\eta$ plane is the crystal facet, where the ζ-axis is along the normal direction of it, and the $\zeta\eta$ plane is the incident plane. For uniaxial crystal, two of its three principle dielectric functions are equal, which can be represented by $\varepsilon_\perp$ and $\varepsilon_\parallel$, respectively, and the dielectric tensor of it in the laboratory coordinate system can be written as [1]:

$$\varepsilon_{ij} = \sum_{k=1}^{3}\sum_{l=1}^{3}\alpha_{ki}\,\alpha_{lj}\,, \tag{5}$$

where $\varepsilon_{ij}(i,j=1,2,3)$is the component of dielectric tensor in the laboratory coordinate system o-$\xi\eta\zeta$ and $\alpha_{ij}(i,j=1,2,3)$is the component of coordinate transformation matrix between the laboratory coordinate system and principal axis coordinate system. Three most common situations are considered here: (i) The optical axis is along the normal direction of crystal facet (As $c \parallel \zeta$, i.e., $\delta = 0°$). (ii) The optical axis is the intersection line between the incident plane and crystal facet (As $c \parallel \eta$, i.e., $\delta = 90°$ $\varphi = 90°$). (iii) The optical axis is perpendicular to the incident plane (As $c \parallel \xi$, i.e., $\delta = 90°$ $\varphi = 0°$). (ii) and (iii) are both suitable for the *m*- and *a*-plane of uniaxial crystals, but the difference between them is that when the optical axis is in the incident plane, that is, situation (ii), the two refracted rays propagating in the crystal are in a same plane; but when the optical axis is not in the incident plane, such as situation (iii), the two refracted rays are not in a same plane [30].

For the three situations above, it can be found that there are two kinds of refracted rays known as ordinary ray (*o* ray) and extraordinary ray (*e* ray) corresponding to two different dielectric functions in uniaxial crystals [30, 31]:

$$\varepsilon_{\mathbf{or}}(\omega) = \varepsilon_\perp(\omega), \tag{6}$$

$$\varepsilon_{ex}(\omega,\theta) = \frac{\varepsilon_\perp(\omega)\varepsilon_\parallel(\omega)}{\varepsilon_\perp(\omega)\,\sin^2\theta + \varepsilon_\parallel(\omega)\,\cos^2\theta}, \tag{7}$$

where θ is the angle between the refracted wave vector and the optical axis (refer Supplemental Information for more details). That is to say, two different refracted rays, namely, *o* ray and *e* ray, will propagate in the uniaxial crystals when the light beam is incident to the crystal facet and the reflection occurs, which means that contribution from these two refracted rays should be taken differently into consideration when calculating the interface reflectance. Because of the birefringence in uniaxial crystals, we no longer use R_s and R_p to represent the interface reflectance as we do in the case of optically isotropic crystals, but note the corresponding interface reflectance as R_{or} and R_{ex} for *o* and *e* rays, respectively. Remarkably, the refractive properties of *o* ray are similar to those of optically isotropic crystals, so R_{or} can still be calculated by Eqs. (2) and (3) while R_{ex} can only be obtained from the continuous conditions of the electromagnetic field at the boundary between the uniaxial crystal and air because the refractive properties of e ray are related to its propagating direction. Table 1 summarizes (refer Supplemental Information for more details) the interface reflectance formulas corresponding to *o* ray and *e* ray of those three specific cases [32, 33].

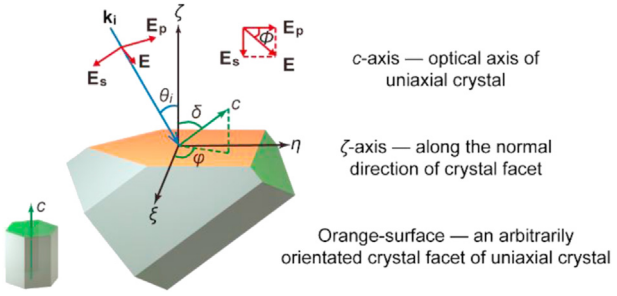

Figure 2. Experimental geometry configuration of polarized IR reflectance measurement. For uniaxial crystal, the crystal *c*-axis is its optical axis. A fixed laboratory coordinate system o - $\xi\eta\zeta$ is established on the crystal facet measured in the experiment. The $\xi\eta$ plane is the crystal facet, the ζ-axis is along the normal direction of it, and the $\zeta\eta$ plane is the incident plane. The linearly polarized light is incident from air with an angle θ_i to an arbitrarily orientated crystal facet, and its electric field vector **E** forms an angle ϕ with the incident plane. The angle between the optical axis and the ζ-axis is δ and the azimuth angle of the projection of optical axis in the $\xi\eta$ plane is φ.

For uniaxial crystal, considering the anisotropy of the dielectric function, the dielectric function expressed in Eq. (1) should be written as [29, 31]:

$$\varepsilon_{\perp(\parallel)} = \varepsilon_{\infty\perp(\parallel)} + \frac{\omega^2_{TO\perp(\parallel)}(\varepsilon_s - \varepsilon_\infty)_{\perp(\parallel)}}{\left(\omega^2_{TO\perp(\parallel)} - \omega^2 - i\omega\gamma_{\perp(\parallel)}\right)}. \tag{8}$$

When the incident angle θ_i is 10°, the reststrahlen band of AlN in three situations is predicted through Eq. (8), as shown in Figure 3(a-c). Based on the optical anisotropy of AlN, specific parameters used in this model are ω_{TO} (⊥) = 670 cm^{-1}, γ_{TO} (⊥) = 5.2 cm^{-1}, ε_s (⊥) = 7.28, ε_∞(⊥) = 3.93 for $\varepsilon_\perp$ and ω_{TO} (∥) = 611 cm^{-1}, γ_{TO} (∥) = 6.7 cm^{-1}, ε_s (∥) = 8.59, ε_∞(∥) = 4.54 for $\varepsilon_\parallel$, contributed by E_1 and A_1 phonons, respectively [28, 29].

It can be observed that there are no additional peaks in the reststrahlen band corresponding to *o* ray, but on the contrary, extra peaks appear in the reststrahlen band corresponding to *e* ray, which is similar to that of experiment results. For wurtzite crystals, the principle dielectric functions $\varepsilon_\parallel$ and $\varepsilon_\perp$ are contributed from A_1 phonon which is polarized along the optical axis and E_1 phonon which is polarized in the plane perpendicular to the optical axis, respectively [29]. Previous studies have shown that there is a directional dispersion in uniaxial crystals, that is to say, the dielectric function depends only on the frequency ω and the direction of the wave vector **k** of the refracted ray [11]. For *o* ray, its dielectric function ε_{or} (ω) is a constant value, which is contributed by pure E_1 phonon and independent of the direction of **k**. Therefore, when *o* ray propagates in the crystal, the pure E_1 (TO) phonon is coupled with photon to form phonon polaritons. But when *e* ray propagates in the crystal, the dielectric function ε_{ex} (ω, θ) is related to the direction of **k** and directional dispersion will occur in ε_{ex} (ω,θ). Accordingly, the symmetry of the optical phonon will disappear and a new mix-symmetry phonon, namely, quasiphonon, will generate.

In order to observe how pure A_1 mode and E_1 mode phonon contribute to the quasiphonon, the phonon energy loss function Im (-1/ε) and the imaginary parts of the dielectric function Im(ε) of *e* ray, which show the component of LO phonon and TO phonon, respectively [10, 29, 34], are shown in Figure 4. It can be seen that when *e* ray propagates in the crystal with the long-range electrostatic force being dominant, the symmetry of A_1 (TO) and E_1 (TO) phonons disappears to form the mix-symmetry quasi-TO phonon [35, 36], of which the frequency can be described as [12, 37]:

$$\omega^2_{quasi-TO} = \omega^2_{A1(TO)}\sin^2\sigma + \omega^2_{E1(TO)}\,{}^2\sigma, \tag{9}$$

where σ is the angle between the phonon wave vector **q** and the optical axis. When the frequency of photon coincides with that of quasi-TO phonon, they couple with together and thus the quasiphonon polaritons generates. That is to say, when *e* ray propagates in optically anisotropic wurtzite crystals, the reststrahlen band mainly results from quasiphonon polaritons [38]; also, a characteristic peak formed by the superposition of A_1 (LO) and E_1 (LO) phonons can be observed on the high-frequency side of the band since the LO phonons still maintains the symmetry of A_1 and E_1 at this time.

Figure 3 also shows the reflectance R_{mix} corresponding to natural light. Since the natural light is non-polarized, R_{mix} is the result of all kinds

Table 1. Interface reflectance corresponding to *o*-ray, *e*-ray and non-polarized natural light of uniaxial crystals under various conditions. Optical axis is along the normal direction of crystal facet ($c \parallel \zeta$). Optical axis is the intersection line between the incident plane and crystal facet ($c \parallel \eta$). Optical axis is perpendicular to the incident plane ($c \parallel \xi$).

Reflectance	$c \parallel \zeta$	$c \parallel \eta$	$c \parallel \xi$
R_{or}	$\left\|\frac{\cos\theta_i - \sqrt{\varepsilon_\perp - \sin^2\theta_i}}{\cos\theta_i + \sqrt{\varepsilon_\perp - \sin^2\theta_i}}\right\|^2$	$\left\|\frac{\cos\theta_i - \sqrt{\varepsilon_\perp - \sin^2\theta_i}}{\cos\theta_i + \sqrt{\varepsilon_\perp - \sin^2\theta_i}}\right\|^2$	$\left\|\frac{\cos\theta_i - \sqrt{\frac{\varepsilon_\perp - \sin^2\theta_i}{\varepsilon_\perp{}^2}}}{\cos\theta_i + \sqrt{\frac{\varepsilon_\perp - \sin^2\theta_i}{\varepsilon_\perp{}^2}}}\right\|^2$
R_{ex}	$\left\|\frac{\cos\theta_i - \sqrt{\frac{\varepsilon_\parallel - \sin^2\theta_i}{\varepsilon_\perp\varepsilon_\parallel}}}{\cos\theta_i + \sqrt{\frac{\varepsilon_\parallel - \sin^2\theta_i}{\varepsilon_\perp\varepsilon_\parallel}}}\right\|^2$	$\left\|\frac{\cos\theta_i - \sqrt{\frac{\varepsilon_\perp - \sin^2\theta_i}{\varepsilon_\parallel\varepsilon_\perp}}}{\cos\theta_i + \sqrt{\frac{\varepsilon_\perp - \sin^2\theta_i}{\varepsilon_\parallel\varepsilon_\perp}}}\right\|^2$	$\left\|\frac{\cos\theta_i - \sqrt{\varepsilon_\parallel - \sin^2\theta_i}}{\cos\theta_i + \sqrt{\varepsilon_\parallel - \sin^2\theta_i}}\right\|^2$
R_{mix}	$(R_{or} + R_{ex})/2$		

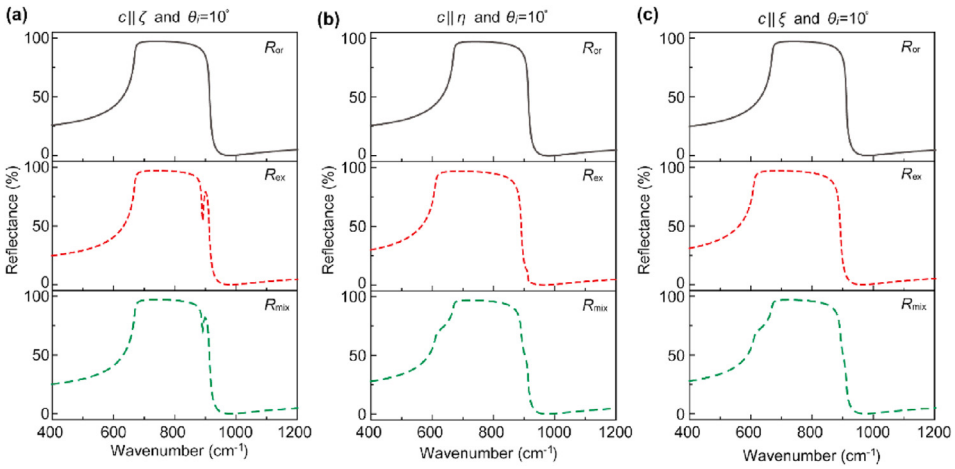

Figure 3. Theoretical results of the reststrahlen band of AlN in three situations when the incident angle $\theta_i$is 10° according to quasiphonon-polaritons model (refer Supplemental Information for other cases where the incident angle takes values such as 0°, 30°and 60°). (a) Optical axis is along the normal direction of crystal facet (As $c \parallel \zeta$, i.e., $\delta = 0°$). (b) Optical axis is the intersection line between the incident plane and crystal facet (As $c \parallel \eta$, i.e., $\delta = 90°$ $\varphi = 90°$). (c) Optical axis is perpendicular to the incident plane (As $c \parallel \xi$, i.e., $\delta = 90°$ $\varphi = 0°$).

of polarized state, that is, R_{mix} is the combination of R_{or} and R_{ex} and thus additional characteristic peaks can be found at the high- and low-frequency ends of the reststrahlen band, respectively.

The reststrahlen band described by the quasiphonon-polaritons model is shown in Figure 1(b) (the red short-dashed lines), from which it can be observed that the theoretical curves show adequate information of the hump- and spike-shaped peaks and agree well with the experimental data. This is because this model has taken the optical anisotropy shown by AlN as a uniaxial crystal and the existence of quasiphonons in its wurtzite structure into consideration comprehensively. At this time, the original phonon polaritons "mutate" into quasiphonon polaritons in the crystals, which implies the failure of the original phonon-polaritons model in its application to optically anisotropic crystals.

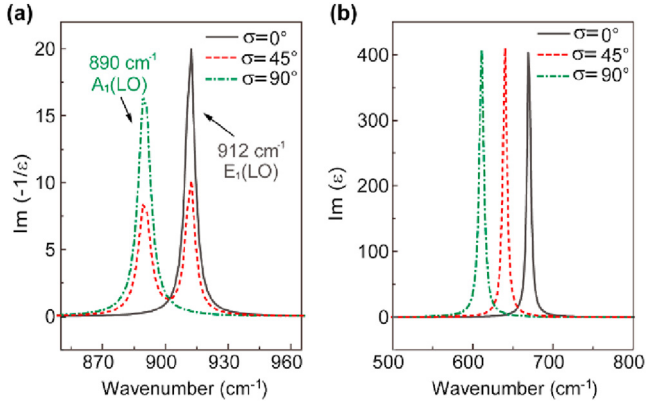

Figure 4. Phonon energy loss function and the imaginary parts of the dielectric function of *e* ray. (a) Phonon energy loss function Im (-1/ε); (b) Imaginary parts of the dielectric function Im(ε).

The dispersion relation of phonon polaritons in optically anisotropic uniaxial crystals has been derived in detail [17, 18, 27]:

$$\frac{c^2k^2}{\omega^2} = \varepsilon_\perp(\omega)(\text{ordinary polaritons}), \tag{10}$$

$$\frac{c^2k^2}{\omega^2} = \frac{\varepsilon_\perp(\omega)\varepsilon_\parallel(\omega)}{\varepsilon_\perp(\omega)\sin^2\sigma + \varepsilon_\parallel(\omega)\cos^2\sigma}\ (\text{extraordinary polaritons}). \tag{11}$$

It can be seen that in uniaxial crystal, the dielectric function of refracted light has the same expression as the dispersion relation of phonon polaritons, which means that polaritons are formed by the coupling between refraction light and phonon and then further propagate in the crystal. Therefore, the direction of the wave vector **k** of refracted light should be consistent with that **q** of the polaritons, i.e. $\sigma = \theta$. It is worth pointing out that in the Raman studies, the polaritons related to quasiphonon are known as "extraordinary polaritons" [37, 39, 40], corresponding to the "quasiphonon polaritons" discussed here.

Finally, it should be pointed out that, the reflectivity measured in the experiment is the total reflectivity where gold mirror used as reference rather than the actual interface reflectance. There are some differences between them but the error will not affect the final result. Besides, here we only take AlN as an example to discuss the quasiphonon polaritons in wurtzite crystals, and this result needs to be further extended to other wurtzite crystal materials.

4. Conclusions

In this work, a quasiphonon-polaritons model is proposed based on the analysis of the extra hump-and spike-shaped peaks appearing on the reststrahlen band of wurtzite crystals. According to this model, these

extra peaks are attributed to the quasiphonon polaritons generating from the coupling between quasi-TO phonon and photon in the crystals with the long-range electrostatic forces being dominant. Related formulas are given here, and the reststrahlen band related to quasiphonon polaritons in AlN measured in the experiment is well explained, which proves the validity of this new quasiphonon-polaritons model. Additionally, a series of reststrahlen band under different experimental configurations is predicted to cast a new light on the future studies about optically anisotropic wurtzite crystals.

Declarations

Author contribution statement

Lu Cheng: Conceived and designed the experiments; Performed the experiments; Analyzed and interpreted the data; Wrote the paper.

Wei Zheng: Conceived and designed the experiments; Analyzed and interpreted the data; Contributed reagents, materials, analysis tools or data; Wrote the paper.

Lemin Jia, Feng Huang: Contributed reagents, materials, analysis tools or data.

Funding statement

Feng Huang was supported by National Natural Science Foundation of China (91333207, 61427901, 61604178, 91833301, U1505252).

Competing interest statement

The authors declare no conflict of interest.

Additional information

Supplementary content related to this article has been published online at https://doi.org/10.1016/j.heliyon.2020.e05277.

References

[1] C.S. Smith, Macroscopic symmetry and properties of crystals, in: Advances in Research and Applications, 1958, pp. 175–249.
[2] M. Born, E. Wolf, Principles of Optics : Electromagnetic Theory of Propagation, Interference and Diffraction of Light, seventh ed., University Press,Cambridge, United Kingdom, 2003.
[3] J. Lekner, Reflection and refraction by uniaxial crystals, Condens. Matter. 3 (1991) 6121–6133.
[4] S.C. Lee, et al., Crystal orientation dependence of polarized infrared reflectance response of hexagonal sapphire crystal, Opt. Mater. 37 (2014) 773–779.
[5] Y. Zhu, et al., Near vacuum-ultraviolet aperiodic oscillation emission of AlN films, Sci. Bull. 65 (10) (2020) 827–831.
[6] Y. Zhu, et al., Deep-ultraviolet aperiodic-oscillation emission of AlGaN films, Opt. Lett. 45 (7) (2020) 1719–1721.
[7] Joshua D. Caldwell, et al., Low-loss, infrared and terahertz nanophotonics using surface phonon polaritons, Nanophotonics 4 (1) (2015) 44–68.
[8] K. Huang, On the interaction between the radiation field and ionic crystals, Proc Roy Soc A 208 (1094) (1951) 352–365.
[9] M. Born, K. Huang, Dynamical Theory of Crystal Lattices, Clarendon Press, Oxfold, 1954.
[10] A.S. Barker, M. Ilegems, Infrared lattice vibrations and free-electron dispersion in GaN, Phys. Rev. B 7 (2) (1973) 743–750.
[11] F. Engelbrecht, R. Helbig, Effect of crystal anisotropy on the infrared reflectivity of 6H-SiC, Phys. Rev. B 48 (21) (1993) 15698–15707.
[12] C.A. Arguello, D.L. Rousseau, S.P.S. Porto, First-order Raman effect in wurtzite-type crystals, Phy. Rev. 181 (3) (1969) 1351–1363.
[13] W. Zheng, et al., Raman tensor of AlN bulk single crystal, Photon. Res. 3 (2) (2015).
[14] J.F. Scott, S.P.S. Porto, Longitudinal and transverse optical lattice vibrations in quartz, Phy. Rev. 161 (3) (1967) 903–910.
[15] Leah Bergman, et al., Raman analysis of the E1 and A1 quasi-longitudinal optical and quasi-transverse optical modes in wurtzite AlN, J. Appl. Phys. 85 (7) (1999) 3535–3539.
[16] M. Bickermann, et al., Orientation-dependent phonon observation in single-crystalline aluminum nitride, Appl. Phys. Lett. 86 (13) (2005).
[17] G. Irmer, et al., Raman tensor elements and Faust-Henry coefficients of wurtzite-type α-GaN: how to overcome the dilemma of the sign of Faust-Henry coefficients in α-GaN? J. Appl. Phys. 116 (24) (2014).
[18] R. Loudon, The Raman effect in crystals, Adv. Phys. 13 (52) (1964) 423–482.
[19] L. Jia, et al., Ultra-high photovoltage (2.45 V) forming in graphene heterojunction via quasi-fermi level splitting enhanced effect, iScience 23 (2) (2020) 100818.
[20] R. Lin, et al., X-ray radiation excited ultralong (>20,000 seconds) intrinsic phosphorescence in aluminum nitride single-crystal scintillators, Nat. Commun. 11 (1) (2020) 4351.
[21] W. Zheng, et al., Vacuum ultraviolet photovoltaic arrays, Photon. Res. 7 (1) (2018).
[22] W. Zheng, et al., Vacuum-Ultraviolet photovoltaic detector with improved response speed and responsivity via heating annihilation trap state mechanism, Adv. Optic. Mater. 6 (21) (2018).
[23] W. Zheng, L. Jia, F. Huang, Vacuum-Ultraviolet photon detections, iScience 23 (6) (2020) 101145.
[24] W. Zheng, et al., Vacuum-Ultraviolet photovoltaic detector, ACS Nano 12 (1) (2018) 425–431.
[25] L. Cheng, et al., Ultra-wide spectral range (0.4–8 μm) transparent conductive ZnO bulk single crystals: a leading runner for mid-infrared optoelectronics, Mater. Today Phy. 14 (2020).
[26] A.S. Barker, Transverse and longitudinal optic mode study in MgF2and ZnF2, Phys. Rev. 136 (5A) (1964) A1290–A1295.
[27] J.F. Scott, Light scattering from polaritons, Am. J. Phys. 39 (11) (1971) 1360–1372.
[28] V.Y. Davydov, et al., Phonon dispersion and Raman scattering in hexagonal GaN and AlN, Phys. Rev. B 58 (1998) 12899–12907.
[29] M. Kazan, et al., Directional dependence of AlN intrinsic complex dielectric function, optical phonon lifetimes, and decay channels measured by polarized infrared reflectivity, J. Appl. Phys. 106 (2009), 023523.
[30] E. Hecht, Optics, fourth ed., Wesley, San Francisco, 2001.
[31] L. Merten, G. Lamprech, Directional dependence of etraodinary infrared oscillator parameters of uniaxial crystals (I), Phys. Status Solidi B 39 (2) (1970) 573–580.
[32] F. Wooten, Refletivity of uniaxial absorbing crystals, Appl. Optic. 23 (1984) 4226–4227.
[33] L.P., Mosteller JR., F. Wooten, Optical properties and reflectance of uniaxial absorbing crystals, J. Opt. Soc. Am. 58 (1968) 511–518.
[34] J. Onstott, G. Lucovsky, Directional dispersion of extraordinary optical phonons in α-quartz in the frequency domain from 380 to 640cm−1, J. Phys. Chem. Solid. 31 (10) (1970) 2171–2184.
[35] B.C. Lee, K.W. Kim, Electron–optical-phonon scattering in wurtzite crystals, Phys. Rev. B 56 (1997) 997–1000.
[36] M.E. Mora-Ramos, F.J. Rodríguez, L. Quiroga, Polaron properties of III-V nitride compounds- second-order effects, J. Phys. Condens. Matter 11 (1999).
[37] G. Irmer, et al., Phonon polaritons in uniaxial crystals, Phys. Rev. B 88 (2013) 104303.
[38] L. Merten, G. Borstel, Bulk and surface phonon polaritons in anisotropic crystals, J. Raman Spectrosc. 10 (1) (1981) 205.
[39] M.C.S. Laval, Stimulated extraordinary polaritons in a-quartz, Phys. Status Solidi 71 (1) (1975) 197–205.
[40] D.L. Mills, E. Burstein, Polaritons, The electromagnetic modes of media, Rep. Prog. Phys. 37 (1974) 817–926.